ACS OMEGA

Open Access

http://pubs.acs.org/journal/acsodf

Article

Heterogeneous Mn@CeO$_2$ Catalyst for α-Alkylation of Ketones with Alcohols via Hydrogen-Borrowing Strategy

Rajagopal Swaathy and Sambantham Karthikeyan*

Cite This: *ACS Omega* 2025, 10, 9649−9660

Read Online

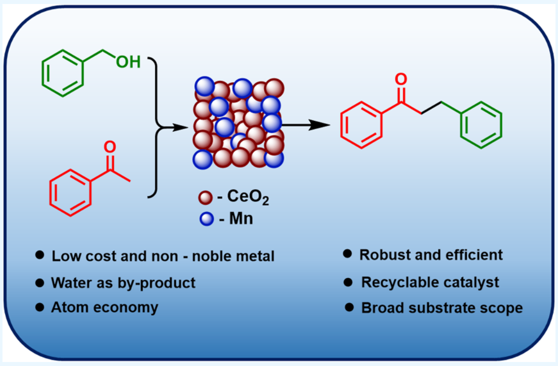

ABSTRACT: Construction of a C-C bond via alkylation of ketones with alcohol as the alkylating source by employing hydrogen-borrowing strategy is attracting significant attention and is highly appealing due to its simplicity, cost-effectiveness, environmental benefits, and the fact that water is the only byproduct. The development of heterogeneous catalysts based on nonprecious base metals is progressing rapidly. Our newly disclosed manganese-doped cerium oxide nanocomposite (10 wt % Mn@CeO$_2$) stands out as a cost-efficient and air-stable catalyst, synthesized through a straightforward coprecipitation method and employed for α-alkylation of ketones with primary alcohols via the hydrogen-borrowing strategy. X-ray diffraction (XRD) analysis confirms the high crystallinity of CeO$_2$, while field emission scanning electron microscopy (FE-SEM) and high-resolution transmission electron microscopy (HR-TEM) images reveal MnO$_2$ nanoparticles, measuring 19 nm in size, uniformly decorated on the rod-shaped CeO$_2$ nanoparticles, which have a size of 33 nm. X-ray photoelectron spectroscopy (XPS) analysis uncovers the presence of Mn^{4+} species embedded on the CeO$_2$ nanorods. Electron paramagnetic resonance (EPR) analysis further indicates that surface defects contribute to the impressive catalytic yield, which ranges from 70 to 98% for the α-alkylated ketones. Thermogravimetric analysis (TGA) demonstrates the remarkable thermal stability of the catalyst, maintaining its stability up to 800 °C. Additionally, inductively coupled plasma mass spectrometry (ICP-MS) confirms no leaching of Mn ions, emphasizing the high heterogeneity of the catalyst. Remarkably, 10 wt % Mn@CeO$_2$ nanocomposite is recycled for six cycles with no loss of catalytic activity. This study underscores the synergistic effect between the base metal MnO$_2$ and redox pair of CeO$_2$, which is key to the exceptional catalytic activity in α-alkylation reactions, making 10 wt % Mn@CeO$_2$ a highly promising catalyst for sustainable and efficient C-C bond formation.

1. INTRODUCTION

The creation of carbon-carbon bonds is important for organic synthesis. Organic electrophiles or organometallic coupling partners are used in the traditional alkylation process together with stoichiometric bases, which results in a large number of hazardous pollutants.[1] There is a great need to overcome these obstacles and develop an environmentally benign process for forming C-C bonds. Hydrogen autotransfer or hydrogen-borrowing strategy is a simple yet incredibly effective technique that uses alcohol, a commonly available and renewable resource, as the alkylating source. The only byproduct produced by this process is water. As a result, it is sustainable, environmentally friendly, and atom-economical. Preactivation of alcohols is also unnecessary. The α-alkylation of ketones using alcohol as an electrophile is a particularly appealing technique because of its ease of operation. The hydrogen-borrowing strategy involves three steps: (i) dehydrogenation of alcohols to carbonyl compounds; (ii) condensation with acidic C-H to generate an α-β unsaturated product; and (iii) hydrogenation via hydrogen autotransfer (Scheme 1).

Several homogeneous noble metal catalysts such as Ir,[2−9] Ru,[10−17] and Pd[18−21] (Scheme 2i) have been developed for alkylation reactions using the hydrogen-borrowing mechanism. Replacing noble metals with non-noble base metal homogeneous catalysts such as Fe,[22,23] Co,[24,25] Cu,[26] Mn,[27−36] Cr,[37,38] Zn,[39] and Ni[40,41] was also done for hydrogen-borrowing reactions. Similarly, the hydrogen-borrowing strategy was employed for synthesis of *N*-heterocyclic compounds efficiently.[42] Homogeneous catalysts do have certain drawbacks, like the fact that the catalyst is sensitive and can be challenging to separate from the reaction media; also, the reaction requires an inert atmosphere to proceed, and certain complexes must be handled carefully. The inability to be recycled for more than one catalytic cycle is another significant disadvantage of homogeneous catalysts.

Received: December 3, 2024
Revised: January 20, 2025
Accepted: January 29, 2025
Published: February 24, 2025

Scheme 1. Metal-Catalyzed α-Alkylation of Ketones Using the Hydrogen-Borrowing Strategy

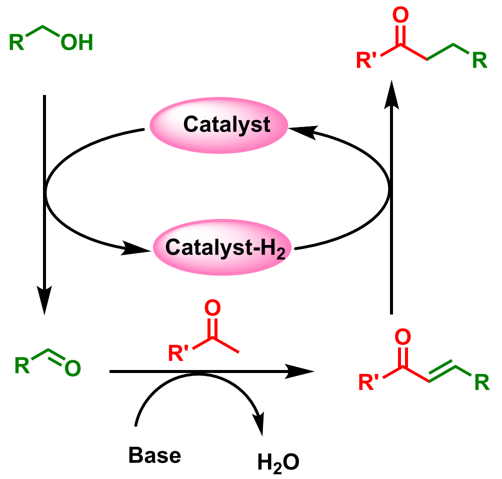

Scheme 2. α-Alkylation of Ketones with Alcohols Via the Hydrogen-Borrowing Strategy

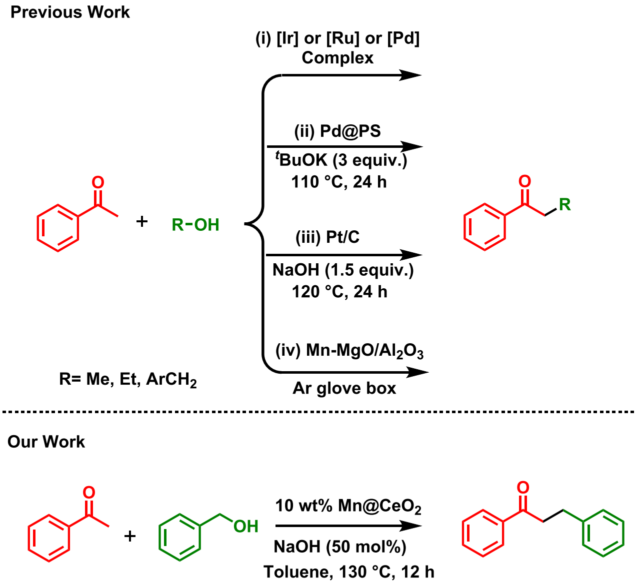

Das's group reported polymer-supported palladium nanoparticles for the α-alkylation of ketones using short-chain and long-chain benzylic and aliphatic alcohols (Scheme 2ii).[43] Shimizu and group reported *C*-methylation of alcohols, ketones, and indoles using methanol with Pt loaded on a carbon catalyst[44] (Scheme 2iii). Kita et al.[45] reported on Ru on MgO/TiO$_2$ support for *N*-alkylation using alcohols. Wang and group used iridium supported on phosphorus-doped porous organic polymers for the hydrogen-borrowing reaction.[46] Wang and group incorporated Ru nanoparticles onto the metal-organic framework support and used it as a heterogeneous catalyst for *N*-alkylation with alcohol.[47] Chen and co-workers synthesized recyclable metal-organic frameworks functionalized with iridium phosphine for *N*-alkylation of amines.[48]

For the alkylation reactions employing the hydrogen-borrowing technique, however, very few heterogeneous catalysts based on non-noble metals have been found. Pathak and group reported Ni(II)-impregnated porous organic polymers as a reusable catalyst for the *N*-alkylation of amines using alcohols.[49] Recently, Nova and group reported a computational study on the single-atom nickel catalyst for the alkylation of amines following the hydrogen-borrowing mechanism.[50] Cai and group synthesized NiP nanoparticles supported on N- and P-codoped carbon material and used them for the alkylation of nitriles with alcohols.[51] Hima and group reported on the hydroxyapatite-supported copper nanocatalyst for the *S*-alkylation of dithiocarbamates with alcohols.[52] Liu and co-workers designed an efficient heterogeneous hybrid material containing a Co-P complex linked on ZIF-8 for *N*-alkylation of anilines with alcohols.[53] Zhang and group reported copper-based mixed oxides for alkylation of ketones with alcohols.[54] Li and group designed the recyclable Cd(II)-coordinated polymer for *N*-alkylation of aminoquinolines using alcohols.[55] Malini and group reported alkylation of ketones and quinoline synthesis using the heterogeneous TiO$_2$ catalyst.[56] Xueping and co-workers synthesized lignin-derived *N*-doped porous carbon along with Zn single atom and used it for the alkylation of ketones.[57] Lu and group reported *N*-alkylation of amines with alcohols using Fe single atom on N,S-doped carbon obtained by PANI-modified ZIF.[58] They also developed zinc single atom doped on carbon support having N,S doping derived by the pyrolysis of ZIF for *N*-alkylation of aromatic amines with alcohols.[59] According to Hara and co-workers,[60] the alkylation of ketones is heterogeneously proceeded with the cobalt catalyst along with MgO and TiO$_2$.

Manganese is a non-noble metal that is inexpensive and biocompatible. It is the third most prevalent metal on the Earth. The objective of utilizing a sustainable alcohol source as the alkylating agent and applying the hydrogen-borrowing technique, utilizing the heterogeneous manganese catalyst for alkylation reactions, is valuable. Manganese-catalyzed C-C and C-N bond formation using alcohols via the hydrogen-borrowing strategy is attracting researchers quite well now-a-days.[61−72] Karak[73] reported the MnO$_2$ nanoflower catalyst along with the base KOH and, recently, Balaraman[74] reported manganese grafted on *N*-doped graphene catalyst for alkylation of amines in the presence of two equivalents of ^{t}BuOK base. Wang[75] and group reported on the polymer-supported MnO$_2$ with one equivalent of NaOH and Dateer[76] synthesized δ-MnO$_2$ nanoparticles for α-alkylation of ketones in the presence of one equivalent of the base ^{t}BuOK. For different catalytic systems, different bases are utilized to yield the highest efficiency; therefore, various bases are compared for our catalytic system to assess their relative effectiveness and performance; as a result, it was found that the NaOH base with only 50 mol % gives the maximum yield of 98% product. Mn-supported MgO/Al$_2$O$_3$ for α-alkylation of ketones was recently reported by Hara[77] (Scheme 2iv). The catalyst shows good activity, but it must be synthesized by heating it with H$_2$ at a high temperature , and the reaction must be carried out in an argon glovebox, which presents a practical challenge. Further research is needed for α-alkylation of ketones employing non-noble heterogeneous metal catalysts.

Manganese-doped cerium oxide is used for oxidative coupling of 2-aminophenol[78] and alkene epoxidation.[79] CeO$_2$ nanoparticles are used to synthesize triazole and tetrazole derivatives.[80] Incorporating metal oxide with other metals generates more active sites due to the defects and oxygen vacancies in the lattices. Especially CeO$_2$ exhibits a unique property due to the redox pair of Ce^{4+} and Ce^{3+} ions. The incorporation of Mn^{4+} ions creates abundant oxygen vacancy, providing more active sites and forming a synergetic effect with Ce ions, thereby enhancing the catalytic property of the reaction.

https://doi.org/10.1021/acsomega.4c10938
ACS Omega 2025, 10, 9649−9660

Because of their fascinating capabilities, which are mostly connected to their superior redox features in conjunction with distinctive metal-support interaction phenomena, cerium-based oxides have been used in a wide range of catalytic applications. Most significantly, the intrinsic properties and interfacial reactivity of the catalyst can be significantly impacted by the fine-tuning of essential connected parameters, such as the size, shape, and electronic state of the catalyst's counterparts. Optimizing the metal-support interfacial phenomena is essential for the creation of selective and active catalytic materials, as certain spots at the interface might offer exceptionally high reactivity.[81]

The primary effects of fine-tuning engineering through either aliovalent doping or suitable synthesis pathways on important activity descriptors are then covered in detail, with the latest ceria-based catalysts for CO_2 hydrogenation serving as examples.[82] Ceria-based catalysts are used for the hydrogenation of CO_2 to CO or CH_4, which exhibits similar or even higher reactivity to noble metal catalysts. The activation of gas-phase CO_2 toward CO or CH_4 can be significantly increased by explicitly fabricating CeO_2-based systems with increased redox capabilities and, consequently, oxygen vacancy abundance. Furthermore, the performance of CO_2 hydrogenation can be significantly impacted by the morphology engineering of CeO_2-based catalysts.

We designed recyclable, air-stable 10 wt % Mn@CeO_2 nanocomposite synthesized through a simple coprecipitation method for α-alkylation of ketones using primary alcohols in the presence of 50 mol % of base NaOH by employing the hydrogen-borrowing strategy.

2. MATERIALS AND METHODS

2.1. Characterization. Powder X-ray diffraction (XRD) analysis was done by a powder X-ray diffractometer model D8 Advance from Bruker, Germany, equipped with a 2.2 KW Cu anode, a ceramic X-ray tube source, and a Lynx eye detector (silicon strip detector technology). The catalyst structure, morphology, and dimension were investigated by FE-SEM (field emission scanning electron microscopy) using the model FEI QUANTA 250 FEG, Thermo Fisher and by scanning electron microscopy (SEM) using a Carl Zeiss model of EVO/18 Research and High Resolution Transmission Electron Microscope (HR-TEM), FEI−TECNAI, G2−20 TWIN (operating voltage 200 kV). Using a 20 min acquisition period, SEM was used to acquire the elemental mapping and for energy dispersive X-ray analysis (EDAX). IRAffinity-1, Shimadzu, Japan, was used to identify the functional groups that were present on the catalyst's surface. The thermal stability and phase transition of the catalyst were examined by thermogravimetric analysis (TGA) using an SDT Q600, TA Instruments, USA, at a heating rate of 10 °C/min. Using an X-ray photoelectron spectrometer (XPS), we investigated the chemical state of the constituents. Quantachrome USA's Brunauer-Emmett-Teller (BET)-surface area analyzer was used to determine both the surface area and pore size. Electron paramagnetic resonance spectroscopy (EPR) was used to analyze the paramagnetic property by utilizing a JEOL Model JES FA200 instrument. Inductively coupled plasma mass spectrometry (ICP-MS) was used to analyze the metal leaching property.

2.2. Synthesis of 10 wt % Mn@CeO_2 Nanocomposite. 10 wt % Mn@CeO_2 catalyst was synthesized by following the previously reported procedure.[83] Aqueous solutions of 0.2 g of $Mn(NO_3)_2{\cdot}H_2O$ and 1 g of $[Ce(NO_3)_6](NH_4)_2$ were combined, and they were stirred for approximately 5 h at 80 °C. After that, the mixture was stirred for an additional 3 h, while aqueous ammonia was added drop by drop until the pH reached 10. Eventually, the precipitate was separated by centrifugation, and to get rid of any impurities and unreacted components, it was repeatedly washed with ethanol and water. The next step was to dry it for 12 h at 120 °C in a hot air oven; the yield was 0.46 g. To obtain the 10 wt % Mn@CeO_2 nanocomposite, it was then calcined at 800 °C with a heating ramp of 5 °C/min in a muffle furnace.

2.3. 10 wt % Mn@CeO_2 Nanocomposite Catalyzed α-Alkylation of Ketones. The following materials were added to a 15 mL screw-capped pressure tube that had been dried in the oven: acetophenone **1a** (0.5 mmol, 1 equiv), benzyl alcohol **2a** (0.5 mmol, 1 equiv), NaOH (0.25 mmol, 50 mol %), 10 wt % Mn@CeO_2 catalyst (10 mg), and toluene (3 mL). Over the course of about 12 h, the reaction was stirred in an oil bath kept at a temperature of 130 °C. TLC was checked for the reaction completion. Filtration was used to remove the catalyst, and then the crude product was concentrated. Using column chromatography, ethyl acetate, and hexane as eluents, the pure product was obtained.

3. RESULTS AND DISCUSSION

A simple coprecipitation technique was used to synthesize 10 wt % Mn@CeO_2. For around 5 h at 80 °C, an aqueous solution containing manganese(II) nitrate hydrate and cerium(IV) ammonium nitrate was stirred. After adding aqueous ammonia dropwise to the homogenized solution until the pH of the solution reached 10, the precipitate was aged for an additional three h at 80 °C. Subsequently, the precipitate underwent centrifugation, ethanol washing, and calcination at 400, 600, and 800 °C. Without using a manganese precursor, bare CeO_2 was synthesized via a similar process. Water was utilized as the solvent in this environmentally friendly approach, which also has the benefit of not requiring any capping agents or surfactants or additives.

3.1. Powder X-ray Diffraction (XRD) Analysis. Powder X-ray diffraction (XRD) was used to determine the structural composition of the synthesized CeO_2 and 10 wt % Mn@CeO_2. On analyzing the XRD pattern of 10 wt % Mn@CeO_2 at 400, 600, and 800 °C, it was discovered (Figure S1) that the crystalline structure is only obtained well when 10 wt % Mn@CeO_2 is calcined at 800 °C. The lattice constant a = 5.4085 Å found in the synthesized CeO_2 nanoparticle and the XRD pattern matches the JCPDS file no. 34−0394. The crystal size is 20 nm, as determined by Debye-Scherrer equation. The Mn ions have replaced some of the Ce ions in the CeO_2 crystal lattice, as seen by the lack of other additional peaks in the Mn-doped CeO_2. The substitution of smaller Mn ions over Ce ions (ionic radius of Mn^{4+} = 0.056 nm and Ce^{4+} = 0.097 nm) generates lattice contraction and distortion, which causes a tiny change in the diffraction pattern of Mn-doped CeO_2[83−85] (Figure 1). The incorporation of Mn^{4+} ions creates high surface defects and decreases the crystalline size, which are responsible for the enhanced activity of the catalyst toward the α-alkylation.

3.2. FT-IR Study. The FT-IR spectrum of the synthesized CeO_2 and 10 wt % Mn@CeO_2 was analyzed. The major absorption band found at 464 cm^{-1} is due to the Ce-O bond of CeO_2, which got slightly shifted to 485 cm^{-1} for 10 wt % Mn@CeO_2 because of lattice replacement of some of the Ce ions with Mn ions. Very little absorption is found at 1390 cm^{-1} owing to the O-H bending vibrations. The symmetric bending of H_2O

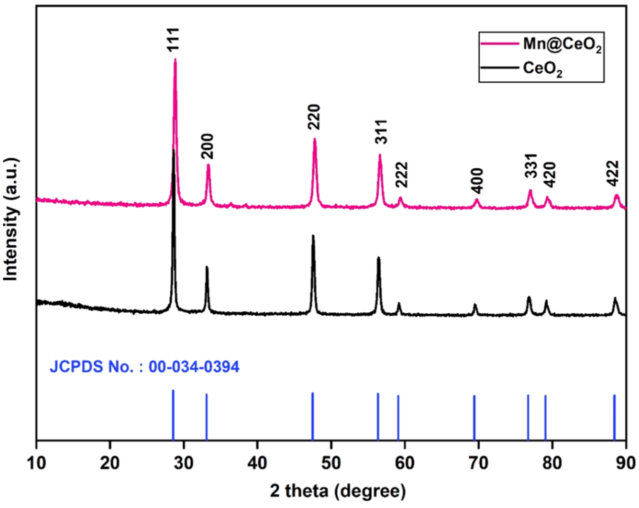

Figure 1. XRD spectra of 10 wt % Mn@CeO$_2$.

exhibits a minute absorption at around 1620 cm^{-1}. The stretching vibration of the O-H molecules of H_2O absorbed on the surface of nanoparticles is represented by the broad minor band around 3406 cm^{-1} (Figure 2).[86]

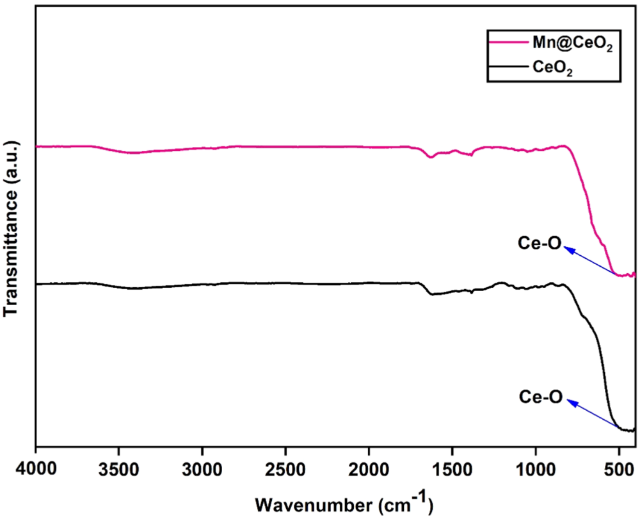

Figure 2. FT-IR spectra of 10 wt % Mn@CeO$_2$.

3.3. Microstructural Analysis. The FE-SEM image shows rod-shaped CeO$_2$ with the diameter of about 33 nm and the manganese nanoparticles are evenly distributed on the CeO$_2$ rods (Figure 3).[87] The consistent distribution of Mn is confirmed by the elemental mapping obtained from SEM (Figure 4a). As for the elemental composition, EDAX analysis reveals that 10 wt % of Mn is doped onto the CeO$_2$ nanoparticle (Figure 4b). Further, the structure and shape of 10 wt % Mn@CeO$_2$ were investigated using HR-TEM analysis, by which we obtained rod-shaped CeO$_2$ with cubic-shaped MnO$_2$ doped onto it (Figure 5a). The *d* spacings between the lattice fringes are approximately 0.69, 0.46, and 0.20 nm corresponding to MnO$_2$ (JCPDS file no. 00-042-1169) (Figure 5b,c). The CeO$_2$ is 33 nm in diameter and the cubic-shaped MnO$_2$ of 19 nm size is obtained from the histogram obtained by HR-TEM (Figure 5d). The concentric circles obtained in the SAED pattern are in good agreement with the XRD results (Figure 5e). The rod-shaped morphology of CeO$_2$ along with the cubical MnO$_2$ helps in increasing the efficiency of the catalyst.

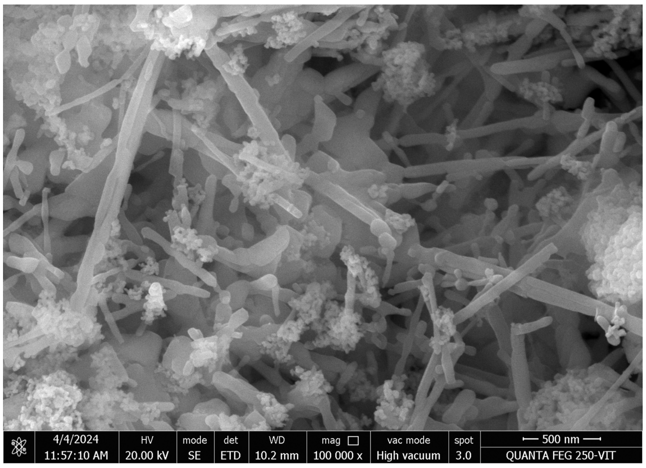

Figure 3. FE-SEM image of 10 wt % Mn@CeO$_2$.

3.4. N$_2$ Sorption Study. Nitrogen sorption isotherms for the synthesized catalyst examined using Brunauer-Emmett-Teller (BET) gave a type (IV) isotherm with empanada-shaped hysteresis (H3 category).[88] With a surface area of 34.454 m^2/g, a pore width of 1.423 nm, and a pore volume of 0.253 cc/g, the BJH pore size distribution reveals that the pores are mesoporous in nature (Figure 6). The mesopores present on the surface of the catalyst facilitate the active sites for the effective alkylation of ketones.

3.5. Thermal Study. Thermogravimetric analysis (TGA) demonstrates that the catalyst does not break down up to 800 °C, and the residue that is recovered is around 99.55%. The catalyst's water molecules are responsible for the tiny loss, which is further supported by differential thermal analysis (DTA) (Figure 7). These findings demonstrate the great stability of 10 wt % Mn@CeO$_2$. The high thermal stability of the catalyst enables the use of the catalyst at high temperature, thereby favoring the product formation.

3.6. X-ray Photoelectron Spectroscopy (XPS). Utilizing X-ray photoelectron spectroscopy (XPS), the oxidation states of the elements were examined. Regarding C 1s, which has a binding energy of 285.0 eV, all binding energies are corrected. The presence of Ce, Mn, O, and C is indicated by the sample's survey spectrum. The peaks at 882.9 and 901.6 eV correspond to the Ce 3d$_{5/2}$ and Ce 3d$_{3/2}$ peaks of CeO$_2$. Table 1 displays the peaks of CeO$_2$.[87] The lattice oxygen is found at the binding energy of 529.8 eV. The Mn 2p spectrum shows two peaks at 642.4 and 653.9 eV indicating the presence of Mn^{4+} species in the catalyst[79] (Figure 8). As revealed by the XPS analysis, the presence of both Mn^{4+} species of MnO$_2$ along with the redox pair of Ce^{3+} and Ce^{4+} species of CeO$_2$ leads to the synergistic effect, exhibiting the best catalytic performance.

3.7. EPR Analysis. Electron paramagnetic resonance spectroscopy (EPR) was used to analyze the surface defects present and the electronic properties of paramagnetic species. The strong EPR signals obtained for the synthesized 10 wt % Mn@CeO$_2$ nanocomposite show the presence of paramagnetic species. The EPR analysis shows that the Mn doping onto CeO$_2$ creates oxygen vacancies, thereby creating surface defects. The strong signals are due to the presence of O^{2-} species on the surface of the catalyst. The presence of high oxygen vacancies on the surface and lattice defects enhances the efficiency of the

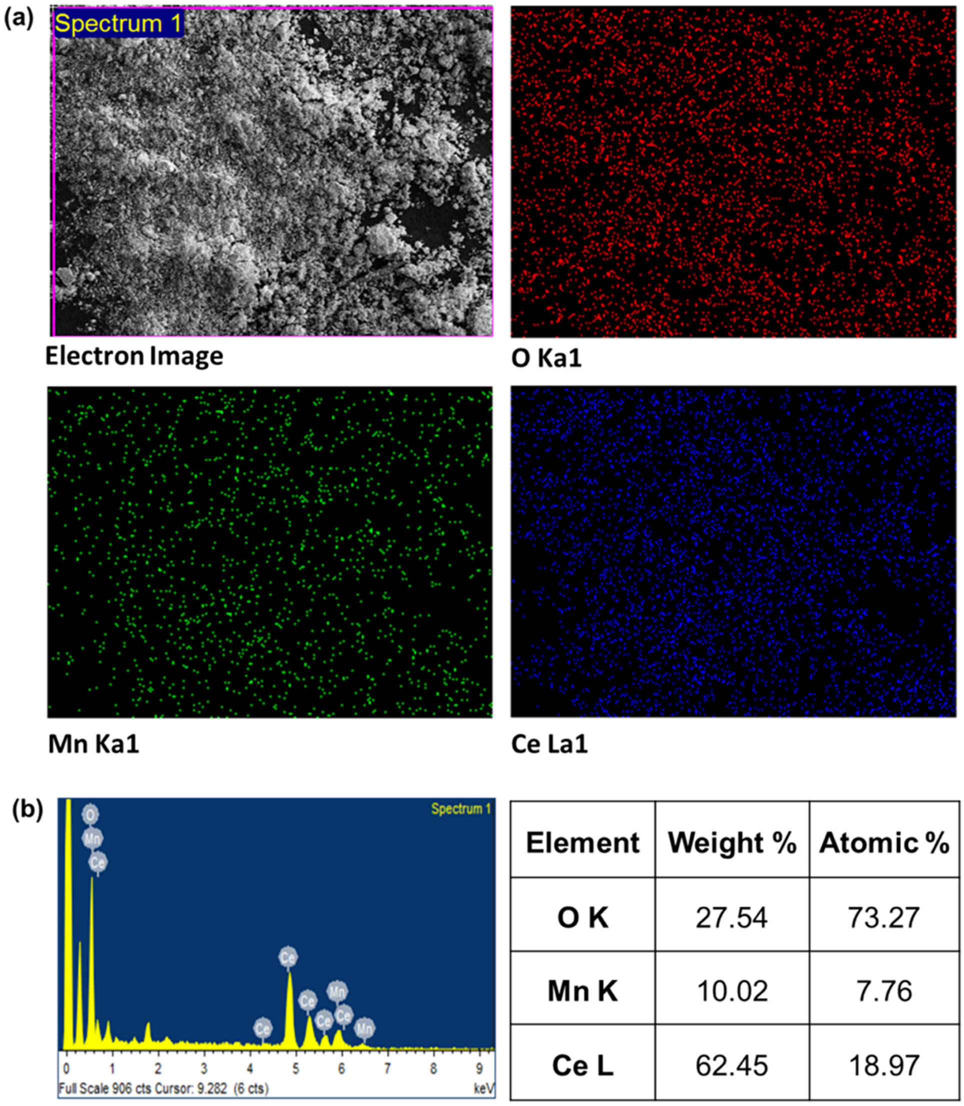

Element	Weight %	Atomic %
O K	27.54	73.27
Mn K	10.02	7.76
Ce L	62.45	18.97

Figure 4. (a) Elemental mapping and (b) EDAX of 10 wt % Mn@CeO$_2$.

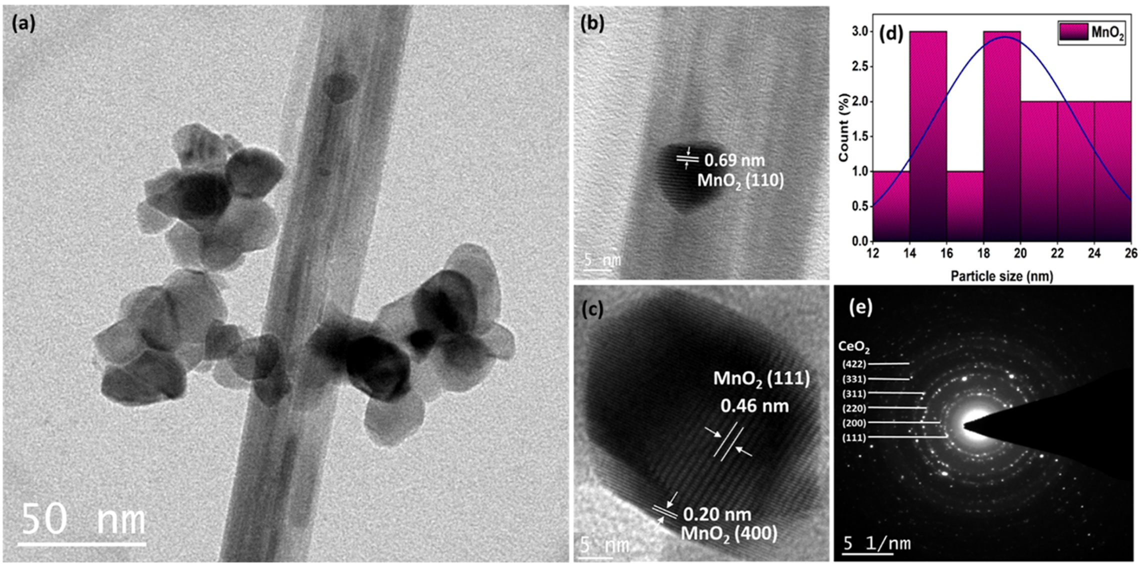

Figure 5. (a)−(c) HR-TEM image of 10 wt % Mn@CeO$_2$. (d) Histogram of MnO$_2$ in 10 wt % Mn@CeO$_2$. (e) SAED pattern of 10 wt % Mn@CeO$_2$.

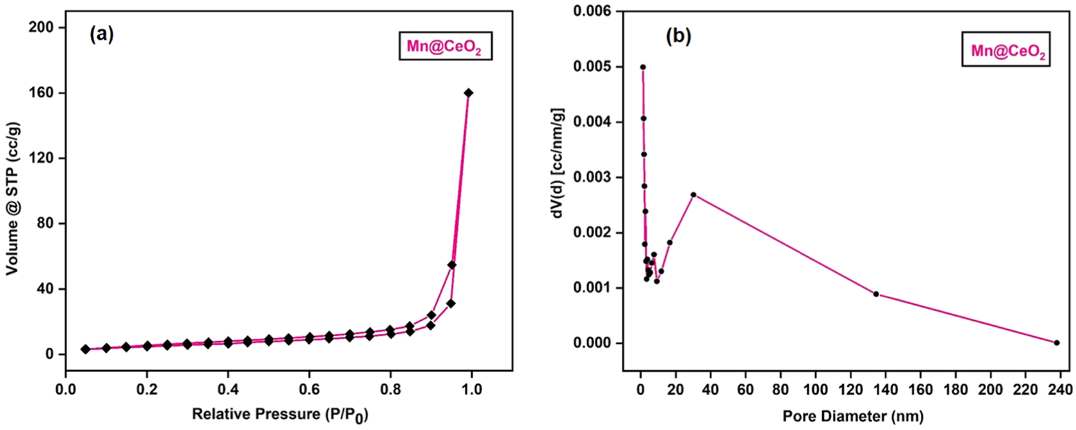

Figure 6. (a) BET isotherm and (b) pore size distribution of 10 wt % Mn@CeO_2.

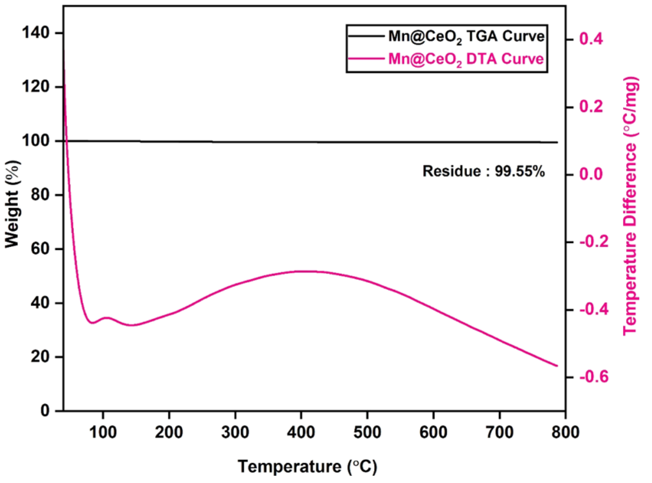

Figure 7. TGA and DTA of 10 wt % Mn@CeO_2.

Table 1. Oxidation State and Binding Energies of Element Cerium

	v_0	v	v′	v″	v‴
Ce 3d5/2					
oxidation state	Ce^{3+}	Ce^{4+}	Ce^{3+}	Ce^{4+}	Ce^{4+}
B.E. (eV)	880.2	882.9	885.9	889.4	898.9
	u	u′	u″	u‴	
Ce 3d3/2					
oxidation state	Ce^{4+}	Ce^{4+}	Ce^{4+}	Ce^{4+}	
B.E. (eV)	901.6		907.8	917.2	

catalyst. Hence, the EPR analysis reveals that the defects present are responsible for the great catalytic activity of the synthesized 10 wt % Mn@CeO_2 nanocomposite[86] (Figure 9).

3.8. Catalysis Study. After the complete characterization of the catalyst 10 wt % Mn@CeO_2, it is used for α-alkylation of ketones with alcohols. Initially we started with the acetophenone (**1a**) and benzyl alcohol (**2a**) as the benchmark substrates for the optimization of the reaction condition. α-Alkylated ketone (**3a**) was produced in 80% yield when the reaction between 1a and 2a was conducted using 10 mg of 10 wt % Mn@CeO_2 catalyst in toluene at 130 °C for 12 h, when 50 mol % of ^{t}BuOK was used (Table 3, Entry 1). The yield of **3a** rises to 98% only in the presence of NaOH, when the reaction is conducted with several bases, including Cs_2CO_3, Na_2CO_3, K_2CO_3, KOH, and NaOH (Table 2, Entry 2−6). Since the reaction did not proceed without a base, it is evident that a base is necessary for the reaction to occur (Table 2, Entry 7). The product **3a** yield abruptly drops to 63% when NaOH is reduced to 25 mol % (Table 2, Entry 8). The yield was marginally reduced to 80% by switching the solvent to 1,4-dioxane (Table 2, Entry 9). Product **3a** was not obtained by using polar solvents such as DMF, THF, and DMSO (Table 2, Entry 10−12). Reducing the duration, from 12 to 6 h, results in a drop in **3a** yield (Table 2, Entry 13). The reaction depends on temperature as well. A drop in temperature causes a progressive loss in yield, while an increase in temperature to 150 °C causes a loss in yield of **3a** because of the generation of byproducts (Table 2, Entry 14−16). When the catalyst was replaced with commercially available MnO_2 and bare CeO_2, there was a significant yield loss, demonstrating the critical role that Mn and Ce ions play in the catalytic system (Table 2, Entry 17−18). Also, we tried the reaction with the manganese precursor, but we did not get the desired yield of the product (Table 2, Entry 19). The absence of a catalyst was shown to have a substantial impact on the poor yield of **3a** (Table 2, Entry 20). The yield of **3a** remains unchanged when the weight percentage of Mn doping onto CeO_2 is increased, but the yield decreases when the Mn doping on CeO_2 is decreased (Table 2, entries 21 and 22).

Following the optimization of the reaction, we investigated α-alkylation using several derivatives of benzyl alcohol (**2a**). The reaction gives a high yield for the electron-donating group (OMe) when present in the para position (**3b**); however due to steric hindrance, the yield slightly decreases when present in the ortho position (**3c**). Similarly, the electron-rich group (Me) present in the meta position gives good yield (**3d**) compared to ortho position (**3e**). The benzyl alcohol with an electron-withdrawing group (**3f**) also generates good yield. The acetophenone (**1a**) also is modified, and the presence of the electron-donating group (OMe) in para position (**3g**) gives excellent yield, but when present in the meta position (**3h**), the yield is decreased. The presence of para-substituted methyl acetophenone gives good yield (**3i**). The electron-withdrawing groups such as Cl and Br acetophenone (**3j** and **3k**) give good yield. When both acetophenone and benzyl alcohol had electron-donating groups (OMe and Me), the product was obtained in moderate to good yield (**3l**−**3q**). By substituting the electron-withdrawing groups (Cl and Br) in acetophenone and an electron-donating OMe group in benzyl alcohol, the product (**3r**−**3u**) was generated in moderate yield (Table 3). We also tried the reactions with aliphatic alcohols and aliphatic ketones.

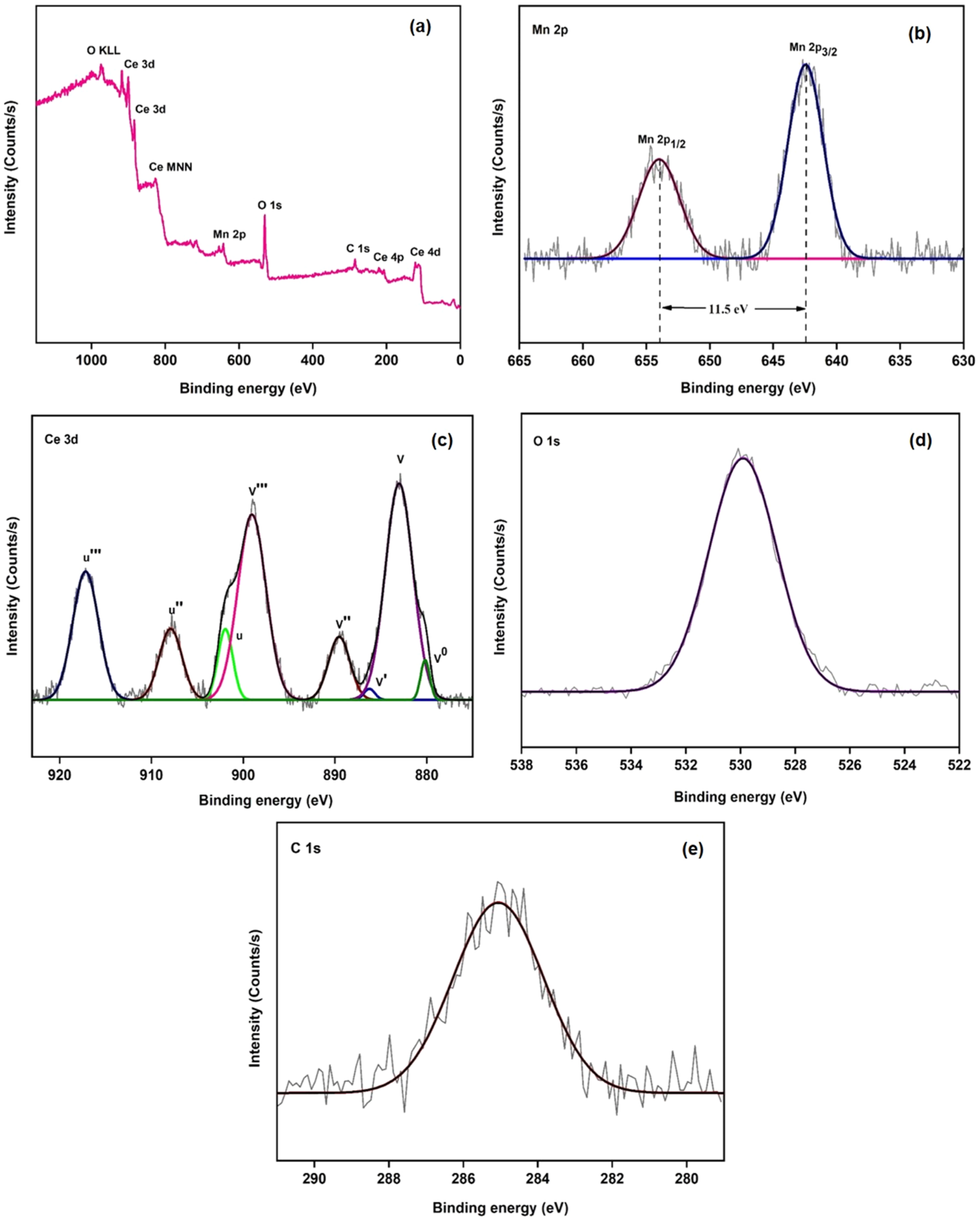

Figure 8. XPS analysis of 10 wt % Mn@CeO_2: (a) survey spectrum, (b) high-resolution Mn 2p spectrum, (c) high-resolution Ce 3d spectrum, (d) high-resolution O 1s spectrum, and (e) high-resolution C 1s spectrum.

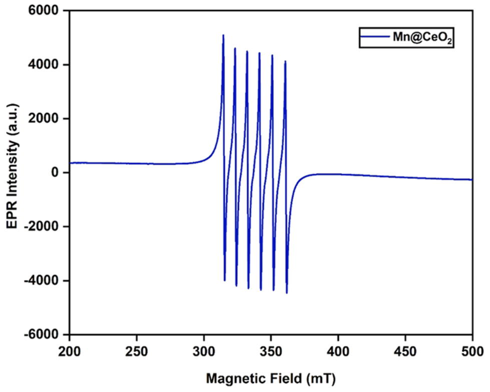

Figure 9. EPR analysis of 10 wt % Mn@CeO_2.

We got product yields less than 10% and 5%, respectively, and hence they cannot be isolated (**3v**−**3x**).

In order to investigate the reaction mechanism, multiple control experiments are conducted (Scheme 3). When acetophenone (**1a**) is absent in the reaction, only in the presence of benzyl alcohol (**2a**) and 10 wt % Mn@CeO_2, dehydrogenation occur, producing hydrogen and aldehyde (Scheme 3a). In the presence of 10 wt % Mn@CeO_2 and acetophenone (**2a**), the aldehyde condenses, creating the unsaturated compound through the Lewis acid sites in the catalyst (Scheme 3b). The alkylated product **3a** is formed finally through hydrogenation, when hydrogen is extracted from the alcohol in the presence of a base (Scheme 3c). We also investigated whether any radical intermediate is formed during the process by carrying out the reaction in the presence of the radical scavenger TEMPO. The product **3a** is formed with good

Table 2. Optimization of Reaction Condition for α-Alkylation of Acetophenone and Benzyl Alcohol

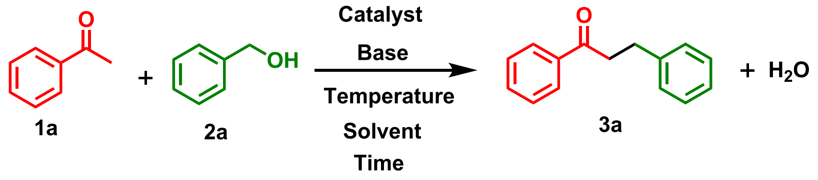

entry[a]	catalyst	solvent	base	time (h)	temp (°C)	yield (%)[b]
1	10 wt % $Mn@CeO_2$	toluene	^{t}BuOk	12	130	80
2	10 wt % $Mn@CeO_2$	toluene	Cs_2CO_3	12	130	n.d
3	10 wt % $Mn@CeO_2$	toluene	Na_2CO_3	12	130	n.d
4	10 wt % $Mn@CeO_2$	toluene	K_2CO_3	12	130	n.d
5	10 wt % $Mn@CeO_2$	toluene	KOH	12	130	50
6	**10 wt % $Mn@CeO_2$**	**toluene**	**NaOH**	**12**	**130**	**98**
7	10 wt % $Mn@CeO_2$	toluene		12	130	n.d
8	10 wt % $Mn@CeO_2$	toluene	NaOH (25 mol %)	12	130	63
9	10 wt % $Mn@CeO_2$	1,4-dioxane	NaOH	12	130	80
10	10 wt % $Mn@CeO_2$	DMF	NaOH	12	130	n.d
11	10 wt % $Mn@CeO_2$	THF	NaOH	12	130	n.d
12	10 wt % $Mn@CeO_2$	DMSO	NaOH	12	130	n.d
13	10 wt % $Mn@CeO_2$	toluene	NaOH	6	130	65
14	10 wt % $Mn@CeO_2$	toluene	NaOH	12	80	50
15	10 wt % $Mn@CeO_2$	toluene	NaOH	12	110	80
16	10 wt % $Mn@CeO_2$	toluene	NaOH	12	150	90
17	MnO_2	toluene	NaOH	12	130	60
18	CeO_2	toluene	NaOH	12	130	40
19	$Mn(NO_3)_2{\cdot}H_2O$	toluene	NaOH	12	130	50
20		toluene	NaOH	12	130	10
21	5 wt % $Mn@CeO_2$	toluene	NaOH	12	130	70
22	20 wt % $Mn@CeO_2$	toluene	NaOH	12	130	98

[a] Reaction condition: Acetophenone **1a** (0.5 mmol, 1 equiv), benzyl alcohol **2a** (0.5 mmol, 1 equiv), base (0.25 mmol, 50 mol %), catalyst (10 mg), solvent (3 mL). [b] GC yield. n.d. not detected.

yield, indicating that the reaction does not proceed through the radical pathway under our reaction conditions. The reaction clearly proceeds by using the method of hydrogen borrowing, as demonstrated by the control experiments.

Our suggested mechanism (Figure 10) serves as a recapitulation of the experiment outcomes. Benzyl alcohol (**2a**) is first adsorbed on the $Mn@CeO_2$ (II) surface and the catalyst removes the hydrogen from the alcohol to create the carbonyl compound (III). Adsorbed on the catalyst (IV), acetophenone (**1a**) experiences condensation with the carbonyl compound owing to the Lewis acid site in $Mn@CeO_2$, which releases water and creates an unsaturated compound (V). The hydrogen adsorbed on the catalyst's surface hydrogenates this compound, resulting in the α-alkylated product, which departs the catalyst for the subsequent catalytic cycle (I).

Six successful cycles of catalyst recycling are achieved by removing the catalyst from the reaction media using a simple filtration process. Product **3a** is produced in good yield after six cycles, demonstrating the persistently good catalytic activity of 10 wt % $Mn@CeO_2$ (Figure 11). It is shown by XRD that the catalyst remains stable even after the sixth cycle (Figure S2).

The catalyst's leaching property is investigated using a hot filtration test (Figure S3). After 6 h of the reaction (**3a** yield 50%), the catalyst is removed and the yield of **3a** does not significantly rise without the catalyst; this indicates the catalyst's pure heterogeneity. Inductively coupled plasma mass spectrometry (ICP-MS) measurement also reveals that there is no manganese leaching from the catalyst. The catalyst can be utilized successfully for more than six cycles without losing any of its catalytic activity.

4. CONCLUSIONS

We have designed the highly air-stable and cost-effective 10 wt% $Mn@CeO_2$ via a straightforward coprecipitation technique, eliminating the need for additives. The synthesized catalyst is well analyzed using various characterization techniques. XRD shows high crystallinity, and a rod-shaped morphology of CeO_2 is found in the FE-SEM. HR-TEM analysis reveals that the cubic MnO_2 of size 19 nm is doped onto the CeO_2 nanorods of 33 nm in diameter. XPS study shows the presence of Mn^{4+} species doped onto the CeO_2 nanorods. TGA analysis exhibits that the synthesized catalyst has high thermal stability up to 800 °C. The surface defects as examined by EPR analysis are responsible for the outstanding catalytic activity. α-Alkylation of ketones with green primary alcohol as the alkylating source was carried out using 10 wt % $Mn@CeO_2$ catalyst. Based on the mechanistic analysis, it can be concluded that the process is environmentally friendly and atom-efficient since it uses the hydrogen-borrowing strategy. A variety of aromatic primary alcohols and a wide spectrum of aromatic ketones having electron-withdrawing and electron-donating groups are readily tolerated by the catalyst; however, aliphatic alcohols and aliphatic ketones could not yield the corresponding product significantly. The synergetic effect of MnO_2 and CeO_2 produced a high yield of about 70−95% of the corresponding α-alkylated product. Leaching study and ICP-MS analysis exhibit that there is no leaching of Mn ions and hence the catalyst is highly heterogeneous in nature. Without

Table 3. 10 wt % Mn@CeO_2-Catalyzed α-Alkylation of Ketone with Primary Alcohol[a,b]

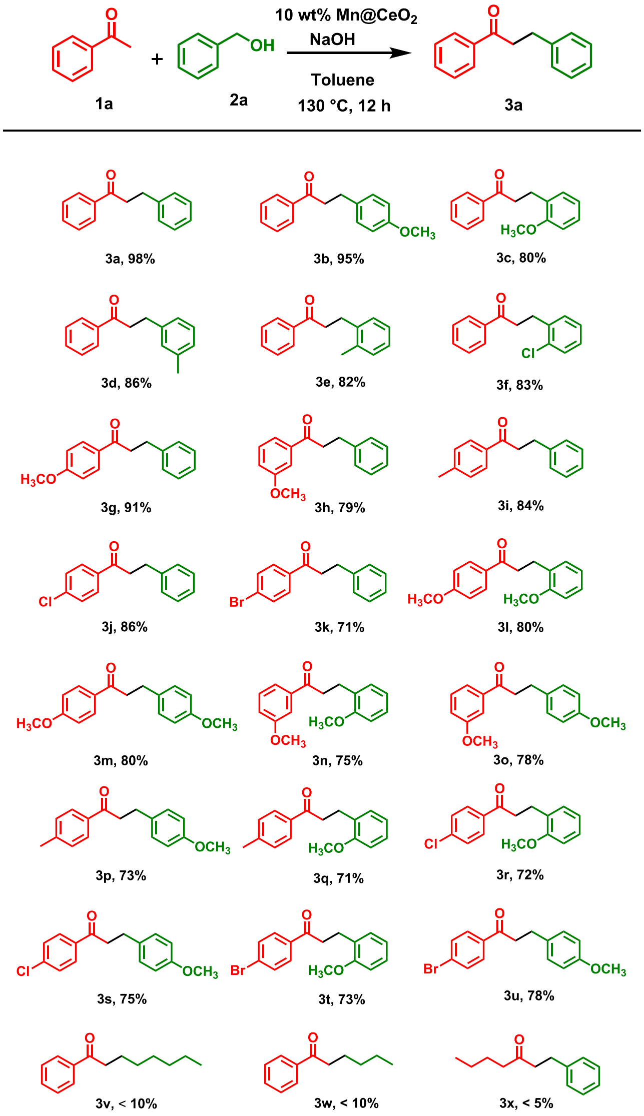

[a]Reaction condition: Acetophenone **1a** (0.5 mmol, 1 equiv), benzyl alcohol **2a** (0.5 mmol,1 equiv), NaOH (0.25 mmol, 50 mol %), 10 wt % Mn@CeO_2 (10 mg), toluene (3 mL), 130 °C, 12 h [b]Isolated yield.

Scheme 3. Control Experiments for α-Alkylation of Ketone with Primary Alcohol[a]

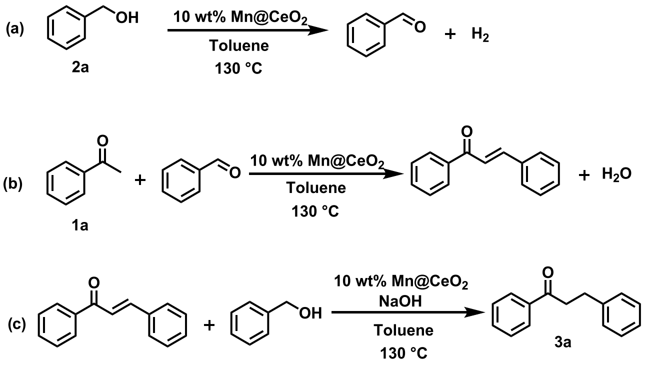

[a](a) Dehydrogenation, (b) condensation, (c) hydrogenation.

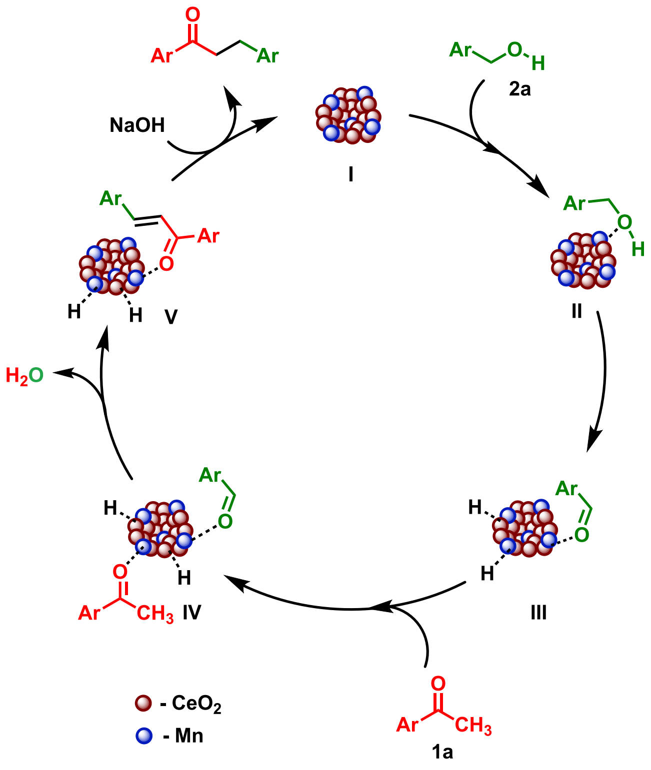

Figure 10. Rationale for the 10 wt % Mn@CeO_2-mediated α-alkylation of ketone with alcohol.

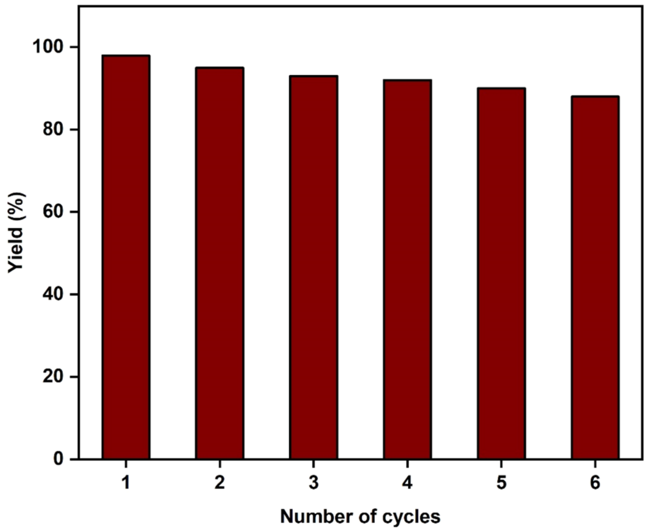

Figure 11. Recyclability test.

sacrificing the catalytic activity, the catalyst can be effectively recovered through a simple filtration method and used over six cycles without significant loss in the yield of the product.

■ ASSOCIATED CONTENT

Supporting Information

The Supporting Information is available free of charge at https://pubs.acs.org/doi/10.1021/acsomega.4c10938.

Additional information as noted in the text, NMR data and spectra (PDF)

■ AUTHOR INFORMATION

Corresponding Author

Sambantham Karthikeyan − *Department of Chemistry, School of Advanced Sciences, Vellore Institute of Technology, Vellore 632014, India*; orcid.org/0000-0001-7807-151X; Email: skarthikeyanphd@vit.ac.in

Author

Rajagopal Swaathy − *Department of Chemistry, School of Advanced Sciences, Vellore Institute of Technology, Vellore 632014, India*

Complete contact information is available at:
https://pubs.acs.org/10.1021/acsomega.4c10938

Notes

The authors declare no competing financial interest.

■ ACKNOWLEDGMENTS

R.S. acknowledges VIT for providing fellowship. R.S. further thanks Dr. Charles Beromeo Bheeter for the initial discussion on this work. The authors acknowledge VIT for seed grants (SG20210184), infrastructures, and instrumental facilities, and UGC-SJSGC fellowship for research funding.

■ REFERENCES

(1) Ayogu, J. I.; Onoabedje, E. A. Recent advances in transition metal-catalysed cross-coupling of (hetero) aryl halides and analogues under ligand-free conditions. *Catal. Sci. Technol.* **2019**, *9* (19), 5233−5255.

(2) Cheang, D. M.; Armstrong, R. J.; Akhtar, W. M.; Donohoe, T. Enantioconvergent alkylation of ketones with racemic secondary alcohols via hydrogen borrowing catalysis. *Chem. Commun.* **2020**, *56* (24), 3543−3546.

(3) Liu, X.; Dong, W.-Z.; Li, Y.; Yu, X.; Wang, W.-H.; Himeda, Y.; Bao, M. Efficient β-alkylation of secondary alcohols to α-substituted ketones catalyzed by functionalized Ir complexes via borrowing hydrogen in water. *Org. Chem. Front.* **2023**, *10* (2), 355−362.

(4) François, J.; Rio, J.; Jeanneau, E.; Perrin, M.-È. L.; Jacolot, M.; Payard, P.-A.; Popowycz, F. Ir−Na cooperativity controls the diastereoselectivity of borrowing hydrogen C−C alkylation on isosorbide: synthesis methodology and mechanistic investigation. *Org. Chem. Front.* **2023**, *10* (19), 4732−4739.

(5) Nimmagadda, S. K.; Kalidindi, S.; Bondigela, S. S.; Korapati, S.; Dasgupta, D.; Malik, N. A.; Rao, P.; Maity, P.; Coombs, J. R.; Hay, M. Development of a Mild and Efficient Process for Ir-Catalyzed *N*-Alkylation of 4-Bromopyridin-2-amine with a Primary Alcohol via Borrowing Hydrogen. *Org. Process Res. Dev.* **2024**, *28* (8), 3414−3422, DOI: 10.1021/acs.oprd.4c00269.

(6) Chen, Y.-S.; Chiu, S.-Y.; Li, C.-Y.; Chen, T.-R.; Chen, J.-D. Ligand effect of cyclometallated iridium (iii) complexes on *N*-alkylation of amines in hydrogen borrowing reactions. *RSC Adv.* **2023**, *13* (45), 31948−31961.

(7) Kim, S. W.; Foker, E. A.; Wolf, W. J.; Woltornist, R. A.; Shemet, A.; McCowen, S.; Simmons, E. M.; Lin, Z.; He, B. L.; Menger, R. α-Alkylation and Asymmetric Transfer Hydrogenation of Tetralone via Hydrogen Borrowing and Dynamic Kinetic Resolution Strategy Using a Single Iridium (III) Complex. *Org. Lett.* **2024**, *26* (15), 3103−3108.

(8) Bakibillah, M.; Reja, S.; Sarkar, K.; Mukherjee, D.; Das, R. K. Selective catalytic synthesis of α-alkylated ketones and β-alkylated secondary alcohols via hydrogen-borrowing. *New J. Chem.* **2023**, *47* (29), 13655−13660.

(9) Furukawa, S.; Morishima, N.; Fujita, K. I. Low-Temperature *N*-Alkylation of Amines with Alcohols in Protic Solvents Catalyzed by Iridium Complexes Bearing *N*-Heterocyclic Carbenes. *Eur. J. Org. Chem.* **2024**, *27* (6), No. e202301105.

(10) Wang, K.; Zhang, L.; Tang, W.; Sun, H.; Xue, D.; Lei, M.; Xiao, J.; Wang, C. Asymmetric Guerbet reaction to access chiral alcohols. *Angew. Chem., Int. Ed.* **2020**, *132* (28), 11505−11512.

(11) Ng, T. W.; Liao, G.; Lau, K. K.; Pan, H. J.; Zhao, Y. Room-Temperature Guerbet Reaction with Unprecedented Catalytic Efficiency and Enantioselectivity. *Angew. Chem., Int. Ed.* **2020**, *132* (28), 11480−11485.

(12) Thiyagarajan, S.; Gunanathan, C. Catalytic cross-coupling of secondary alcohols. *J. Am. Chem. Soc.* **2019**, *141* (9), 3822−3827.

(13) Thiyagarajan, S.; Vijaya Sankar, R.; Gunanathan, C. Ruthenium-catalyzed α-alkylation of ketones using secondary alcohols to β-disubstituted ketones. *Org. Lett.* **2020**, *22* (20), 7879−7884.

(14) Patel, B.; Ranjan, R.; Chauhan, N. R.; Mukhopadhyay, S.; Choudhury, A. R.; Vyas, K. M. *N*-coordinated Ru (ii) catalyzed solvent free *N*-alkylation of primary amines with alcohols through borrowing hydrogen strategy. *New J. Chem.* **2023**, *47* (17), 8305−8317.

(15) Tsuge, K.; Kubota, S.; Sakamoto, K.; Kitayama, K.; Nishimura, T. Ruthenium-catalysed *N*-alkylation of anilines with primary carbohydrate alcohols via borrowing hydrogen strategy. *Chem. Commun.* **2023**, *59* (46), 7052−7055.

(16) François, J.; Jacolot, M.; Popowycz, F. Borrowing hydrogen C-alkylation with secondary saturated heterocyclic alcohols. *Org. Biomol. Chem.* **2024**, *22*, 4502−4507, DOI: 10.1039/D4OB00543K.

(17) Vijayapritha, S.; Nithya, P.; Viswanathamurthi, P.; Raju, S.; Linert, W. Efficient ruthenium (II) complex catalyzed *N*-alkylation of amines and β-alkylation of secondary alcohol via borrowing hydrogen methodology. *Polyhedron* **2023**, *235*, No. 116351.

(18) Sekar, P. K.; Rengan, R.; Sundarraman, B. NNO Pincer-Supported Pd (II)-Catalyzed Reductive *N*-Alkylation of Challenging Nitroarenes with Alcohols via Borrowing Hydrogen Strategy. *J. Org. Chem.* **2024**, *89* (16), 11161−11172, DOI: 10.1021/acs.joc.4c00621.

(19) Kavin, S. P.; Ramesh, R. Synthesis and structure of Pd (II) pincer complexes: catalytic application in β-alkylation of secondary alcohols involving sequential dehydrogenation of alcohols via the borrowing hydrogen approach. *Dalton Trans.* **2023**, *52* (29), 10038−10044.

(20) Anandaraj, P.; Ramesh, R. *N*-alkylation of benzamides/sulfonamides using alcohols via borrowing hydrogen approach by well-defined Pd (II) pincer complexes. *Appl. Organomet. Chem.* **2023**, *37* (10), No. e7228.

(21) Chaudhary, V. K.; Kukreti, P.; Sharma, K.; Kumar, K.; Singh, S.; Kumari, S.; Ghosh, K. A sustainable strategic approach for *N*-alkylation of amines with activation of alcohols triggered via a hydrogen auto-transfer reaction using a Pd (ii) complex: evidence for metal−ligand cooperativity. *Dalton Trans.* **2024**, *53* (20), 8740−8749.

(22) Song, D.; Wang, S.; Huang, W.; Chen, R.; Hu, F.; Cheng, L.; Zhao, X.; Ling, F.; Zhong, W. Blue-light induced iron-catalyzed chemoselective α-alkylation and α-olefination of arylacetonitriles with alcohols. *Org. Chem. Front.* **2023**, *10* (23), 5908−5915.

(23) Quintil, G.; Diebold, L.; Fadel, G.; Pécaut, J.; Philouze, C.; Clémancey, M.; Blondin, G.; Bjornsson, R.; Quintard, A.; Kochem, A. CO to Isonitrile Substitution in Iron Cyclopentadienone Complexes: A Class of Active Iron Catalysts for Borrowing Hydrogen Strategies. *ACS Catal.* **2024**, *14* (10), 7795−7805.

(24) Siddique, M.; Boity, B.; Rit, A. Control over borrowing hydrogen and acceptorless dehydrogenative coupling process for the Co (iii)−NHC catalysed chemoselective alkylation and cyclisation of 1, 2-phenylenediamine with alcohols. *Catal. Sci. Technol.* **2023**, *13* (24), 7172−7180.

(25) Zhu, B.; Tian, H.; Zhang, Z.; Li, T.; Qu, L.; Tang, C. Cobalt-catalyzed chemoselective alkenylation and alkylation of C (sp3)−H bond in methyl heteroarenes. *J. Catal.* **2024**, *435*, No. 115569.

(26) Xia, Q.; Miao, Y.; Hu, Y.; Xie, Y.; Luo, J. Copper-Catalyzed Borrowing Hydrogen Reaction for α-Alkylation of Amides with Alcohols. *J. Org. Chem.* **2024**, *89* (13), 9654−9660, DOI: 10.1021/acs.joc.4c00404.

(27) Mondal, A.; Kumar, R.; Suresh, A. K.; Sahoo, M. K.; Balaraman, E. Divergence in CH alkylation of indoles under Mn catalysis. *Catal. Sci. Technol.* **2023**, *13* (19), 5745−5756.

(28) Rong, Q.; Li, X.; Sun, N.; Hu, B.; Hu, X.; Jin, L. Phosphine-Free NNN-Manganese (II) Catalyzed *C*-alkylation of Methyl *N*-Heteroarenes via Borrowing Hydrogen. *Adv. Synth. Catal.* **2024**, *366* (7), 1531−1537.

(29) Verma, A.; Elias, A. J. Manganese-catalyzed α-alkylation of sulfones using alcohols via a hydrogen-borrowing strategy: Synthesis of branched sulfones. *Asian J. Org. Chem.* **2024**, *13* (8), No. e202400161.

(30) Pham, H. H.; Nguyen, T. T.; Donnadieu, B.; Hollis, T. K. Synthesis of a CCC-NHC pincer Mn complex: An earth abundant catalyst for synthesis of α-alkylated ketones, 2-oxindole derivatives via borrowing hydrogen and one-pot synthesis of quinolines. *Tetrahedron* **2024**, *163*, No. 134156.

(31) Kulyabin, P. S.; Magdysyuk, O. V.; Naden, A. B.; Dawson, D. M.; Pancholi, K.; Walker, M.; Vassalli, M.; Kumar, A. Manganese-Catalyzed Synthesis of Polyketones Using Hydrogen-Borrowing Approach. *ACS Catal.* **2024**, *14* (14), 10624−10634.

(32) Tang, Q.; Song, D.; Zhang, K.; Mao, W.; Zhao, X.; Du, D.; Ling, F.; Zhong, W. Development of an imidazole-based N, *N*-bidentate ligand for the manganese catalyzed direct coupling of nitriles with alcohols. *RSC Adv.* **2024**, *14* (19), 12978−12982.

(33) Rana, J.; Gupta, V.; Balaraman, E. Manganese-catalyzed direct C−C coupling of α-C−H bonds of amides and esters with alcohols via hydrogen autotransfer. *Dalton Trans.* **2019**, *48* (21), 7094−7099.

(34) Landge, V. G.; Mondal, A.; Kumar, V.; Nandakumar, A.; Balaraman, E. Manganese catalyzed *N*-alkylation of anilines with alcohols: ligand enabled selectivity. *Org. Biomol. Chem.* **2018**, *16* (43), 8175−8180.

(35) Rana, J.; Nagarasu, P.; Subaramanian, M.; Mondal, A.; Madhu, V.; Balaraman, E. Manganese-catalyzed C (α)-alkylation of oxindoles with secondary alcohols via borrowing hydrogen. *Organometallics* **2021**, *40* (6), 627−634.

(36) Yadav, V.; Landge, V. G.; Subaramanian, M.; Balaraman, E. Manganese-catalyzed α-olefination of nitriles with secondary alcohols. *ACS Catal.* **2020**, *10* (2), 947−954.

(37) Wei, D.; Feng, B.; Chen, Q.; Yue, W.; Wang, Y.; Peng, Z. CrCl 2-catalyzed α-alkylation of carbonyl compounds via a borrowing hydrogen approach. *Org. Chem. Front.* **2024**, *11* (7), 1955−1962.

(38) Su, P.; Chen, Z.; Ni, J.; Yang, Z.; Li, Y.; Ke, Z. Surmounting Alkoxide Trap Strategy: *N*-Heterocyclic Carbene Chromium (0)-Catalyzed *C*-Alkylation between Alcohols. *ACS Catal.* **2023**, *13* (19), 12481−12493.

(39) Jana, D.; Roy, S.; Naskar, S.; Halder, S.; Kanrar, G.; Pramanik, K. Potent pincer-zinc catalyzed homogeneous α-alkylation and Friedländer quinoline synthesis reaction of secondary alcohols/ketones with primary alcohols. *Org. Biomol. Chem.* **2024**, *22*, 6393−6408, DOI: 10.1039/D4OB00988F.

(40) Chakraborty, G.; Pal, S.; Chakraborty, S.; Paul, N. D. Erratum-Nickel-Catalyzed Sustainable and Selective Alkylation of Alcohols to α-Alkylated Ketones via Borrowing Hydrogen Approach. *Synlett* **2023**, *34* (06), No. e2.

(41) Subaramanian, M.; Gouda, C.; Roy, T. K.; Ganesan, S.; Banerjee, S.; Vanka, K.; Balaraman, E. Dehydrogenative Coupling of Alcohols with Internal Alkynes under Nickel Catalysis: An Access to β-Deuterated Branched Ketones. *ACS Catal.* **2024**, *14*, 8294−8309.

(42) Sun, K.; Shan, H.; Lu, G. P.; Cai, C.; Beller, M. Synthesis of *N*-Heterocycles via Oxidant-Free Dehydrocyclization of Alcohols Using Heterogeneous Catalysts. *Angew. Chem., Int. Ed.* **2021**, *133* (48), 25392−25406.

(43) Reddy, C. B.; Bharti, R.; Kumar, S.; Das, P. Supported palladium nanoparticle catalyzed α-alkylation of ketones using alcohols as alkylating agents. *ACS Sustainable Chem. Eng.* **2017**, *5* (11), 9683−9691.

(44) Siddiki, S. H.; Touchy, A. S.; Jamil, M. A.; Toyao, T.; Shimizu, K. I. C-methylation of alcohols, ketones, and indoles with methanol using heterogeneous platinum catalysts. *ACS Catal.* **2018**, *8* (4), 3091−3103.

(45) Kita, Y.; Kuwabara, M.; Yamadera, S.; Kamata, K.; Hara, M. Effects of ruthenium hydride species on primary amine synthesis by direct amination of alcohols over a heterogeneous Ru catalyst. *Chem. Sci.* **2020**, *11* (36), 9884−9890.

(46) Yao, W.; Duan, Z. C.; Zhang, Y.; Sang, X.; Xia, X. F.; Wang, D. Iridium Supported on Phosphorus-Doped Porous Organic Polymers: Active and Recyclable Catalyst for Acceptorless Dehydrogenation and Borrowing Hydrogen Reaction. *Adv. Synth. Catal.* **2019**, *361* (24), 5695−5703.

(47) Li, J.; Ou, S.; Sang, X.; Chai, R.; Wang, D. Highly dispersed ruthenium capsulated in UiO-66-NH 2 for hydrogen-borrowing-mediated *N*-alkylation reactions. *Catal. Sci. Technol.* **2024**, *14* (7), 1958−1966.

(48) Chen, W.; Sohail, M.; Veeranna, Y.; Yang, Y.; Bengali, A. A.; Zhou, H.-C.; Madrahimov, S. T. *N*-Alkylation through the Borrowing Hydrogen Pathway Catalyzed by the Metal−Organic Framework-Supported Iridium−Monophosphine Complex. *ACS Appl. Mater. Interfaces* **2024**, DOI: 10.1021/acsami.4c02143.

(49) Pathak, D.; Kumar Kalita, B.; Sharma, H.; Biswakarma, N.; Deka, R. C.; Sarma, B. One-Pot *N*-Alkylation of Amines over Ni (II) Embedded Reusable Porous Organic Polymer via Borrowing Hydrogen Strategy. *ChemCatChem.* **2024**, *16* (8), No. e202301399.

(50) Denjean, A. E.; Nova, A.; Balcells, D. Borrowing Hydrogen Mechanism in Amine Alkylation by Single Atom Nickel Catalysts. *ACS Catal.* **2024**, *14*, 11332−11342.

(51) Su, T.; Wang, J.; Cai, C. Ni2P Nanoparticles Supported on N, P Co-Doped Carbon as Catalyst for α-Alkylation of Arylacetonitriles with Alcohols. *ACS Appl. Nano Mater.* **2024**, *7* (8), 8914−8925.

(52) Hima, P.; Hati, S.; Dey, R. *S*-Alkylation of dithiocarbamates via a hydrogen borrowing reaction strategy using alcohols as alkylating agents. *Org. Biomol. Chem.* **2023**, *21* (31), 6360−6367.

(53) Liu, H.; Tian, L.; Zhang, Z.; Wang, L.; Li, J.; Liang, X.; Zhuang, J.; Yin, H.; Yang, D.; Zhao, G. Atomic-Level Asymmetric Tuning of the Co1−N3P1 Catalyst for Highly Efficient *N*-Alkylation of Amines with Alcohols. *J. Am. Chem. Soc.* **2024**, *146* (29), 20518−20529, DOI: 10.1021/jacs.4c07197.

(54) Zhang, L.; Yao, D.; Wang, X.; Zhang, D. Efficient Cu-Based Mixed Oxides Catalyst for α-Alkylation of Ketones with Alcohols. *Asian J. Org. Chem.* **2024**, *13* (11), No. e202400350.

(55) Li, J.; Mao, A.; Hu, X.; Wang, L.; Wang, D.; Duan, Z.-C. Preparation of a novel cadmium-containing coordination polymer and catalytic application in the synthesis of *N*-alkylated aminoquinoline derivatives via the borrowing hydrogen approach. *Dalton Trans.* **2024**, *53* (11), 5064−5072.

(56) Kala, K.; Gupta, S.; Bhat, V. T.; Sasidharan, M.; Selvam, P.; Malini, T. P. TiO 2 (P25) nanoparticle catalyzed *C*-alkylation and quinoline synthesis via the borrowing hydrogen method. *New J. Chem.* **2023**, *47* (18), 8751−8758.

(57) Zhang, X.; Lu, G.-P.; Wang, K.; Lin, Y.; Wang, P.; Yi, W. Lignin-derived Zn single atom/N-codoped porous carbon for α-alkylation of aromatic ketones with alcohols via borrowing hydrogen strategy. *Nano Res.* **2022**, *15* (3), 1874−1881.

(58) Lu, G.-P.; Shan, H.; Lin, Y.; Zhang, K.; Zhou, B.; Zhong, Q.; Wang, P. A Fe single atom on N, S-doped carbon catalyst for performing *N*-alkylation of aromatic amines under solvent-free conditions. *J. Mater. Chem. A* **2021**, *9* (44), 25128−25135.

(59) Zhang, X.; Zhang, Q.; Reng, J.; Lin, Y.; Tang, Y.; Liu, G.; Wang, P.; Lu, G.-P. N, S Co-Coordinated Zinc Single-Atom Catalysts for *N*-Alkylation of Aromatic Amines with Alcohols: The Role of S-Doping in the Reaction. *Nanomaterials* **2023**, *13* (3), 445.

(60) Suarsih, E.; Kita, Y.; Kamata, K.; Hara, M. A heterogeneous cobalt catalyst for C−C bond formation by a borrowing hydrogen strategy. *Catal. Sci. Technol.* **2022**, *12* (13), 4113−4117.

(61) Ansari, M. F.; Maurya, A. K.; Kumar, A.; Elangovan, S. Manganese-catalyzed C−C and C−N bond formation with alcohols via borrowing hydrogen or hydrogen auto-transfer. *Beilstein J. Org. Chem.* **2024**, *20* (1), 1111−1166.

(62) Cai, X.; Wei, X.; Huang, M. Recent Developments of Transition-Metal-Catalyzed Cross-Coupling of Nitriles and Alcohols. *ChemistrySelect* **2024**, *9* (32), No. e202402955.

(63) Chandra, P.; Ghosh, T.; Choudhary, N.; Mohammad, A.; Mobin, S. M. Recent advancement in oxidation or acceptorless dehydrogen-

ation of alcohols to valorised products using manganese based catalysts. *Coord. Chem. Rev.* **2020**, *411*, No. 213241.

(64) Wang, Y.; Liu, Q. Manganese-catalyzed dehydrogenative/deoxygenative coupling of alcohols. *Synlett* **2020**, *31* (15), 1464−1473.

(65) Rohit, K.; Radhika, S.; Saranya, S.; Anilkumar, G. Manganese-Catalysed Dehydrogenative Coupling−An Overview. *Adv. Synth. Catal.* **2020**, *362* (8), 1602−1650.

(66) Nad, P.; Mukherjee, A. Acceptorless dehydrogenative coupling reactions by manganese pincer complexes. *Asian J. Org. Chem.* **2021**, *10* (8), 1958−1985.

(67) Reed-Berendt, B. G.; Latham, D. E.; Dambatta, M. B.; Morrill, L. C. Borrowing hydrogen for organic synthesis. *ACS Cent. Sci.* **2021**, *7* (4), 570−585.

(68) Mahato, J.; Das, R.; Saha, T. K. 3d Transition Metal Complexes as Homogeneous Catalysts in *N*-Alkylation Reactions Using Alcohols: A Recent Update. *Tetrahedron* **2024**, *165*, No. 134192.

(69) Mullick, S.; Ghosh, A.; Banerjee, D. Recent advances in cross-coupling of alcohols via borrowing hydrogen catalysis. *Chem. Commun.* **2024**, *60* (30), 4002−4014, DOI: 10.1039/d4cc00003j.

(70) Cook, A.; Newman, S. G. Alcohols as Substrates in Transition-Metal-Catalyzed Arylation, Alkylation, and Related Reactions. *Chem. Rev.* **2024**, *124* (9), 6078−6144.

(71) Irrgang, T.; Kempe, R. 3d-Metal catalyzed *N*-and *C*-alkylation reactions via borrowing hydrogen or hydrogen autotransfer. *Chem. Rev.* **2019**, *119* (4), 2524−2549.

(72) Bailey, E. P.; Donohoe, T. J.; Smith, M. D. Functional group tolerant hydrogen borrowing *C*-alkylation. *Nat. Commun.* **2024**, *15* (1), 5131.

(73) Chaudhuri, H.; Karak, N. Heterostructured hybrid rGO@ α-MnO_2/rGO@ δ-MnO_2 nanoflower: an efficient catalyst for aerobic Solvent-Free *N*-Alkylation reactions and energy storage material. *ChemCatChem.* **2020**, *12* (6), 1617−1629.

(74) Subaramanian, M.; Ramar, P. M.; Sivakumar, G.; Kadam, R. G.; Petr, M.; Zboril, R.; Gawande, M. B.; Balaraman, E. Convenient and Reusable Manganese-Based Nanocatalyst for Amination of Alcohols. *ChemCatChem.* **2021**, *13* (20), 4334−4341.

(75) Qiu, Y.; Zhang, Y.; Jin, L.; Pan, L.; Du, G.; Ye, D.; Wang, D. Immobilization of manganese dioxide nanoparticles on modified poly 2, 4-dichlorostyrene microspheres: a highly efficient and recyclable catalyst for borrowing hydrogen reactions. *Org. Chem. Front.* **2019**, *6* (19), 3420−3427.

(76) Ghosh, A.; Hegde, R. V.; Limaye, A. S.; Thrilokraj, R.; Patil, S. A.; Dateer, R. B. Biogenic Synthesis of δ-MnO_2 Nanoparticles: A Sustainable Approach for *C*-Alkylation and Quinoline synthesis via Acceptorless Dehydrogenation and Borrowing Hydrogen Reactions. *Appl. Organomet. Chem.* **2023**, *37* (7), No. e7119.

(77) Kita, Y.; Kuwabara, M.; Kamata, K.; Hara, M. Heterogeneous Low-Valent Mn Catalysts for α-Alkylation of Ketones with Alcohols through Borrowing Hydrogen Methodology. *ACS Catal.* **2022**, *12* (19), 11767−11775.

(78) Sun, F.; Qin, J.; Cao, X.; Zhang, X.; Tang, X.; Wan, T.; Zhao, J.; Ma, J.; Long, Y. Cerium-Doped Manganese Oxide Catalyst for the Oxidative Coupling Synthesis of Fluorescent 2-Amino-1, 9-dimethyl-3 H-phenoxazin-3-one Using Atmospheric Oxygen. *ACS Sustainable Chem. Eng.* **2022**, *10* (28), 9087−9095.

(79) Dissanayake, S.; Vora, N.; Achola, L.; Dang, Y.; He, J.; Tobin, Z.; Lu, X.; Mirich, A.; Gao, P.-X.; Suib, S. L. Synergistic catalysis by Mn promoted ceria for molecular oxygen assisted epoxidation. *Appl. Catal., B* **2021**, *282*, No. 119573.

(80) Suresh, L.; Kumar, P. S. V.; Vinodkumar, T.; Chandramouli, G. Heterogeneous recyclable nano-CeO_2 catalyst: efficient and eco-friendly synthesis of novel fused triazolo and tetrazolo pyrimidine derivatives in aqueous medium. *RSC Adv.* **2016**, *6* (73), 68788−68797.

(81) Bernal, S.; Calvino, J.; Cauqui, M.; Gatica, J.; Larese, C.; Omil, J. P.; Pintado, J. Some recent results on metal/support interaction effects in NM/CeO_2 (NM: noble metal) catalysts. *Catal. Today* **1999**, *50* (2), 175−206.

(82) De, S.; Dokania, A.; Ramirez, A.; Gascon, J. Advances in the design of heterogeneous catalysts and thermocatalytic processes for CO_2 utilization. *ACS Catal.* **2020**, *10* (23), 14147−14185.

(83) Ghosh, T.; Mohammad, A.; Mobin, S. M. Hybrid cobalt doped-cerium oxide as a multifunctional nanocatalyst for various organic transformations. *ACS Sustainable Chem. Eng.* **2019**, *7* (16), 13746−13763.

(84) Hu, C.; Xia, C.; Wang, F.; Zhou, M.; Yin, P.; Han, X. Synthesis of Mn-doped CeO_2 nanorods and their application as humidity sensors. *Bull. Mater. Sci.* **2011**, *34*, 1033−1037.

(85) Hamidian, K.; Saberian, M. R.; Miri, A.; Sharifi, F.; Sarani, M. Doped and un-doped cerium oxide nanoparticles: Biosynthesis, characterization, and cytotoxic study. *Ceram. Int.* **2021**, *47* (10), 13895−13902.

(86) Murugadoss, G.; Kumar, D. D.; Kumar, M. R.; Venkatesh, N.; Sakthivel, P. Silver decorated CeO_2 nanoparticles for rapid photocatalytic degradation of textile rose bengal dye. *Sci. Rep* **2021**, *11* (1), 1080.

(87) Al-Agel, F. A.; Al-Arfaj, E.; Al-Ghamdi, A. A.; Losovyj, Y.; Bronstein, L. M.; Mahmoud, W. E. A novel recipe to improve the magnetic properties of Mn doped CeO_2 as a room temperature ferromagnetic diluted metal oxide. *J. Magn. Magn. Mater.* **2014**, *360*, 73−79.

(88) Baldovino-Medrano, V. c. G.; Niño-Celis, V.; Isaacs Giraldo, R. Systematic analysis of the nitrogen adsorption−desorption isotherms recorded for a series of materials based on microporous−mesoporous amorphous aluminosilicates using classical methods. *J. Chem. Eng. Data* **2023**, *68* (9), 2512−2528.

https://doi.org/10.1021/acsomega.4c10938